



# Coupling a thermodynamically active ice shelf to a regional simulation of the Weddell Sea

V. Meccia<sup>1</sup>, I. Wainer<sup>1</sup>, M. Tonelli<sup>1</sup>, and E. Curchitser<sup>2</sup>

<sup>1</sup>Oceanographic Institute, University of Sao Paulo, Praca do Oceanografico, 191, Sao Paulo, SP 05508-120, Brazil

<sup>2</sup>Institute of Marine and Coastal Science, Rutgers University, 71 Dudley Rd., New Brunswick, NJ 08901, USA

Correspondence to: I. Wainer (wainer@usp.br)

Received: 7 November 2012 – Published in Geosci. Model Dev. Discuss.: 29 November 2012

Revised: 4 July 2013 – Accepted: 5 July 2013 – Published: 9 August 2013

**Abstract.** A thermodynamically interactive ice shelf cavity parameterization is coupled to the Regional Ocean Model System (ROMS) and is applied to the Southern Ocean domain with enhanced resolution in the Weddell Sea. This implementation is tested in order to assess its degree of improvement to the hydrography (and circulation) of the Weddell Sea. Results show that the inclusion of ice shelf cavities in the model is feasible and somewhat realistic (considering the lack of under-ice observations for validation). Ice shelf–ocean interactions are an important process to be considered in order to obtain realistic hydrographic values under the ice shelf. The model framework presented in this work is a promising tool for analyzing the Southern Ocean’s response to future climate change scenarios.

## 1 Introduction

Wind and buoyancy forcing in the Southern Ocean transfers water between density layers and connects the deep ocean to the surface. In this way, it controls the connection between the lower and upper layers of the global overturning circulation and thereby regulates, together with the North Atlantic, the capacity of the ocean to store and transport heat, carbon and other properties. By exporting waters the Southern Ocean ventilates the vast majority of deep waters in the rest of the world ocean (Rintoul et al., 2012). Therefore, it has a significant impact on climate change and variability as well as on biogeochemical cycles (e.g., carbon and nutrients). It is expected that changes in the Southern Ocean can have global impacts, which makes its realistic three-dimensional

representation in ocean models absolutely vital for future projections.

Since the pioneering work of Deacon (1937), the primary source of the Antarctic Bottom Water (AABW), which is the main water mass in the Southern Ocean responsible for the oceans ventilation, has commonly been placed in the Weddell Sea. This is mainly due to the strong interaction between the atmosphere, ocean and sea ice that takes place in that region (Gill, 1973). In fact, in line with Orsi et al. (1993) and Fahrbach et al. (1995), between 50 and 90 % of the AABW acquires its characteristics in the Weddell Sea.

Several attempts to study the Weddell Sea circulation and water mass formation by means of numerical simulations have been recently undertaken. Most of them consist of analysis of global-scale model outputs concentrated in the region of interest (e.g., Goosse and Fichefet, 1999; Kerr et al., 2009; Renner et al., 2009). However, global ocean circulation models (GCMs) do not usually resolve the high-latitude processes in an adequate way and the characteristics and flow patterns of deep and bottom water often remain unrealistic.

The implementation of regional models in the Weddell Sea has to deal with the significant challenge to adequately represent regional processes such as the significant sea ice, ice shelf–ocean interactions that occur in the region. Beckmann et al. (1999) described a circumpolar regional model for the Southern Ocean including the major sub-ice shelf areas. The ocean circulation component is the hydrostatic primitive equation, rigid-lid, model SPEM (Haidvogel et al., 1991) that was modified to allow for the inclusion of sub-ice shelf cavities. Timmermann et al. (2002a) presented a coupled sea ice–ocean model based on the rigid lid SPEM ocean model and a dynamic–thermodynamic sea ice model.

The major sub-ice cavities were included. They showed that sea ice formation appears as a necessary condition for bottom water production in the Weddell Sea. Timmermann et al. (2002b) applied their previous model to study the interannual variability during 1985 and 1993 and they found a strong correlation between fluctuations of atmospheric forcing and sea ice formation. Matano et al. (2002) implemented the Modular Ocean Model (MOM) in a circumpolar domain to study the circulation of the northwestern Weddell Sea and its interaction with the Scotia Sea. They did not consider the ice shelf cavities and sea ice. Hellmer (2004), applying the coupled sea ice–ocean model presented by Timmermann et al. (2002a) quantified the freshwater originating from melting ice shelf bases. His results show that the freshwater flux due to deep basal melting significantly stabilizes the shelf water column in front of an ice shelf as well as downstream due to advection by the coastal current. More recently, Hellmer et al. (2009) forced the model of Timmermann et al. (2002a) with the atmospheric output of the IPCC (Intergovernmental Panel on Climate Change) 20th century scenario simulation of the coupled atmosphere–sea ice–ocean ECHAM5–MPIOM to study the decadal variability around the Antarctic marginal seas. They found that the strongest signal occurs on the southeastern and western Weddell Sea continental shelves where changes in bottom salinity are initiated by a variable sea ice cover and modification of surface waters near the Greenwich meridian.

There are studies that discuss the circulation under the ice shelves. Jenkins (1991) developed a one-dimensional model in which the ice shelf water plume is treated as a turbulent gravity current. Jenkins (1991) applied the model to a flow line on Ronne Ice Shelf to explain the observed distribution and rate of basal melting and freezing. Jenkins and Holland (2002) applied an isopycnic ocean model to the southern Weddell Sea, in which the Filchner–Ronne Ice Shelf is included, to investigate the buoyancy forced circulation on the continental shelf. Finally, the thermodynamic fluxes between the ice baseline and the ocean was the subject of several papers. Holland and Jenkins (1999) presented a hierarchy of models describing the thermodynamic interaction between the base of an ice shelf and the underlying ocean waters. Beckmann and Goosse (2003) developed a simple parameterization for ice shelf melting and the corresponding fresh water flux in ocean models. Holland et al. (2008) studied the response of idealized ice shelves to a series of ocean warming scenarios.

The previous studies have shown that to obtain a realistic representation of the circulation and water masses formation in the Southern Ocean, it is necessary to take the atmosphere–ocean–ice interactions under serious consideration. Nevertheless, a complete model framework considering a sea ice model coupling and an ice shelf parameterization in a regional ocean model with a free surface is less studied, particularly for climate-scale integrations. While climate-scale integrations of ocean models that include sea ice and ice

shelves are not common, some recent studies are available (Losch, 2008; Hellmer et al., 2012; Timmerman et al., 2012).

This work aims to advance the understanding of the role of sea ice and ice–ocean interactions in the Weddell Sea. In particular the relative importance of ice shelves is studied by means of process oriented numerical simulations applying a circumpolar, free surface, regional model. In order to achieve this, the Regional Ocean Model System (ROMS) coupled to a sea ice model is run in the Southern Ocean with a higher resolution in the Weddell Sea. An ice shelf parameterization is included. This model configuration is integrated for a period of 100 yr. This way, for the first time, ROMS is applied with active sea ice and ice shelf processes for climate-scale integrations.

## 2 Model description

### 2.1 Model configuration and setup

The model used in this study is ROMS, which is a free-surface, terrain-following, hydrostatic primitive equations ocean model (Song and Haidvogel, 1994; Haidvogel et al., 1991, 2008). As discussed in Haidvogel et al. (2008), the computational kernel in ROMS utilizes consistent temporal averaging of the barotropic mode to guarantee both exact conservation and constancy preservation properties for tracers and therefore more accurately resolves barotropic processes, while preventing aliasing of unresolved barotropic signals into the slow baroclinic motions. More details can be found in Sect. 3 of Haidvogel et al. (2008) and Shchepetkin and McWilliams (2005).

Two topographic surfaces must be defined for this model configuration: the bottom of the water column and, where necessary, the depth of the portion of the ice shelf thickness that is below the mean sea level. Bottom topography (Fig. 1a) was constructed combining ETOPO5 (NGDC, 1988) and BEDMAP in which sea floor topography is derived from Smith and Sandwell (1997), ETOPO2 and ETOPO5 (NGDC, 1988). Ice shelf thickness (Fig. 1b) was obtained from the BEDMAP gridded digital model of ice thickness (Lythe et al., 2001). Both surfaces were smoothed with a modified Shapiro filter, which was designed to selectively smooth areas where the changes in the ice thickness or bottom bathymetry are large with respect to the total depth (Wilkin and Hedstrom, 1998). It should be noted that perhaps too much smoothing was applied. In particular at the Amery Ice Shelf.

A periodic circumpolar domain between 83 and 50° S with variable horizontal resolution was constructed (Fig. 1c, d). Zonal resolution (Fig. 1c) gradually increases from 150 to 10 km in the Weddell Sea. Meridional resolution (Fig. 1d) varies approximately between 20 and 110 km, reaching the finest scale at the highest latitudes. The horizontal resolution in the Weddell Sea is approximately between 20 and 50 km.

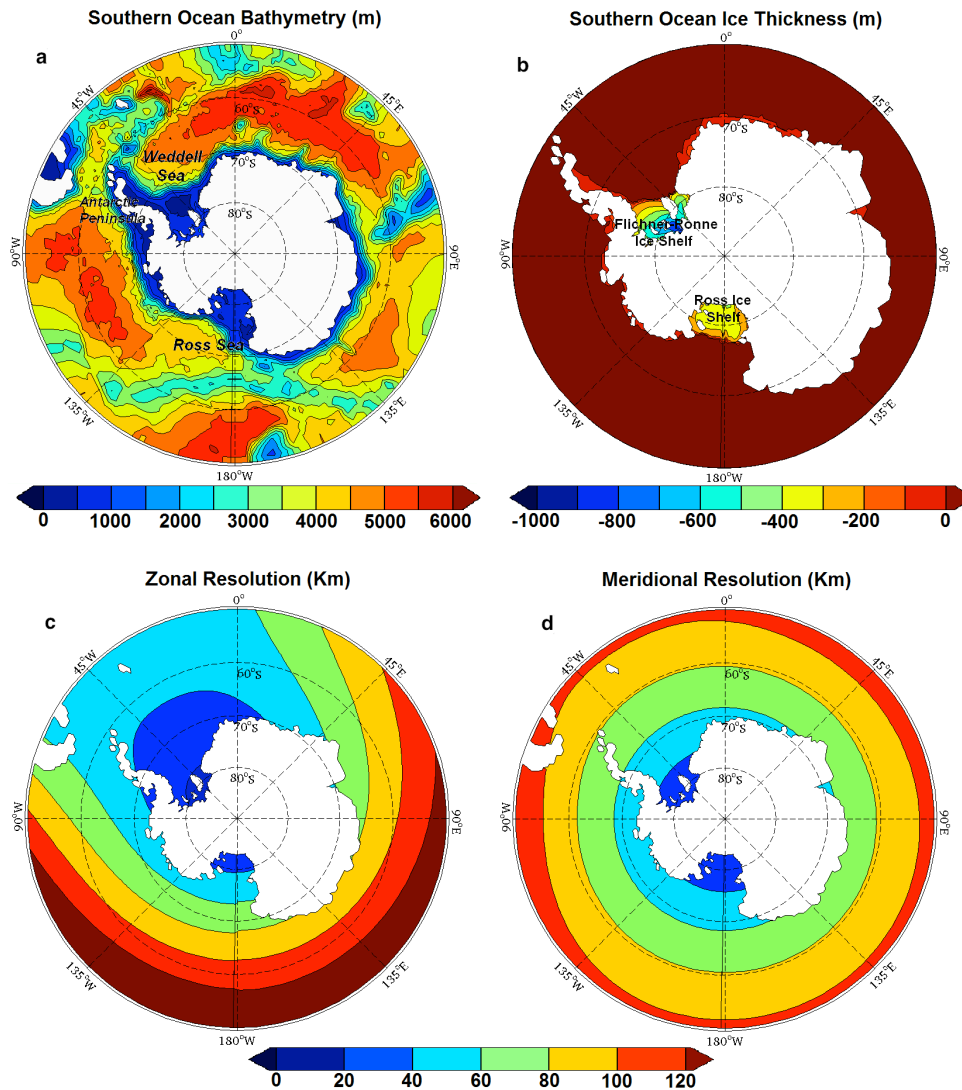


**Fig. 1.** Bathymetry and ice thickness in meters (a and b) and variable horizontal resolution in kilometers (c and d).

In the vertical, 40 terrain-following levels with higher resolution near surface and bottom are used. In this configuration, the model domain contains  $270 \times 70$  grid cells and 40 vertical levels. This grid allows for an efficient and computationally time-effective modeling framework with a higher resolution in the areas of interest.

For the 3-D momentum advection a 4th order centered scheme is applied in the horizontal and in the vertical. For tracers, a 3rd order upstream horizontal and a 4th order centered vertical advection schemes are applied. Biharmonic horizontal mixing of momentum and tracers is used in which the viscosity and diffusivity depend on the grid spacing. Quadratic bottom stress, with a coefficient of  $3.0 \times 10^{-3}$  was applied as a body force over the bottom layer. The vertical momentum and tracer mixing were handled using the KPP (K-Profile Parameterization) mixing scheme. For

computational efficiency, ROMS uses a split-explicit time-stepping scheme in which external (barotropic) and internal (baroclinic) modes are computed separately. The external and internal time steps were set to 0.75 and 30 min, respectively, in compliance with the Courant, Friedrichs and Lewy (CFL) criterion.

A dynamic-thermodynamic sea ice module is coupled to the ocean model, having both of them the same grid (Arakawa-C) and time step and sharing the same parallel coding structure (Budgell, 2005). The sea ice dynamics is based on elastic–viscous–plastic (EVP) rheology (Hunke, 2001). The sea ice thermodynamics follows Mellor and Kantha (1989). Two ice layers and a single snow layer are used in the sea ice module to solve the heat conduction equation. The salt flux underneath the sea ice is a function of the basal melting or freezing, which is controlled by the difference between

the water–sea ice heat flux and the sea ice–atmosphere conductive heat flux.

In addition to sea ice, an ice shelf parameterization is included in order to consider the ice shelf impacts on ocean circulation and water mass formation. The thickness and extent of the ice shelf do not change along the simulations. Under the ice shelves, the upper boundary is no longer at sea level but conforms to the ice shelf base. Below the ice shelves, the atmospheric contributions to the momentum and buoyancy fluxes are set to zero. The heat and salt fluxes are calculated as described in Dinniman et al. (2007) with the modification that the heat and salt transfer coefficients are functions of the friction velocity (Holland and Jenkins, 1999).

The model was initialized by the temperature and salinity fields from the January Levitus World Ocean Data 1998 climatology. Under the ice shelf, specified vertical profiles of temperature and salinity were prescribed as initial conditions. This avoids instabilities produced by the excessive gravity waves at the beginning of the simulation. At the open northern boundary, the model uses the free-surface Chapman condition, the 2-D momentum Flather condition and the 3-D momentum and tracer radiation condition. Temperature and salinity from Levitus 1998 climatology are prescribed as lateral boundary conditions at the open northern boundary.

The atmospheric forcing corresponds to the normal year forcing version 2.0 – COREv2 – (Large and Yeager, 2009). The normal year forcing consists of a single annual cycle of all the data needed to force an ocean model. These data are representative of climatological conditions over decades and can be applied repeatedly for as many years of model integration as necessary (Large and Yeager, 2009; Griffies et al., 2009). It includes a 6-hourly 10 m winds, sea level pressure, 10 m specific humidity and 10 m air temperature; the daily solar shortwave radiation flux and downwelling longwave radiation flux and the monthly precipitation. The air–sea interaction boundary layer is based on the bulk parameterization of Fairall et al. (2003). It was adapted from the Coupled Ocean–Atmosphere Response Experiment (COARE) algorithm for the computation of surface fluxes of momentum, sensible heat and latent heat. Surface salinity is relaxed to Levitus climatology with a timescale of 180 days.

## 2.2 Model simulations

A first simulation with all the cryospheric processes included was run starting from an ocean at rest and integrating the model for 90 yr with a repeated annual cycle forcing. Time series of the annual mean kinetic (red) and potential (blue) energy integrated over the model domain are plotted in Fig. 2a. The annual mean kinetic energy integrated over a horizontal plane is plotted against time and depth in Fig. 2b. It can be observed that the integrated energy is maintained almost constant from year 10 to 90.

In order to address the sensitivity of the regional model to the thermodynamic active ice shelf implementation, an

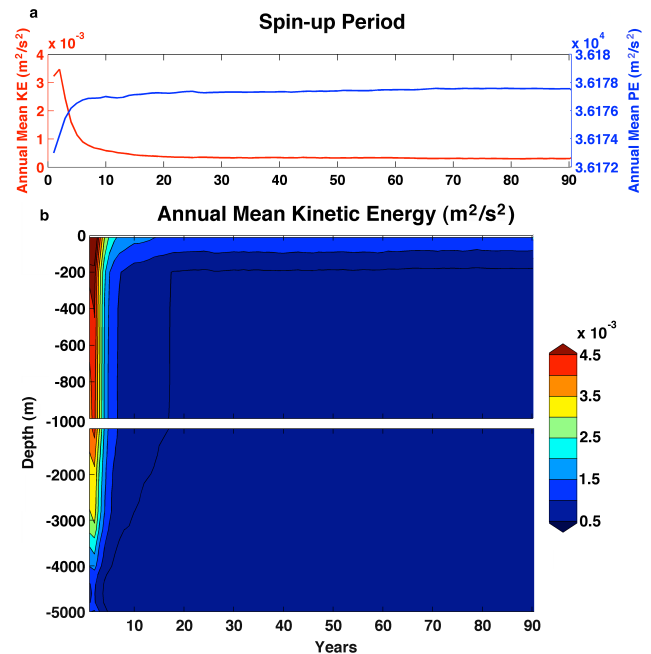


**Fig. 2.** Related to the spin-up period simulation. **(a)** Time series of the annual mean kinetic (red) and potential (blue) energy integrated over the model domain. **(b)** Annual mean kinetic energy integrated over a horizontal plane as a function of time and depth.

additional experiment was conducted after the spin-up period (90 yr) and was run for 10 yr. The first experiment, hereafter named M1, represents the full run with all the complex sea ice and ice shelves physics included. M1 is considered the control run. The second experiment, hereafter named M2, was run to address the effects of the ice shelf inclusion. To run this experiment, the ice shelves were completely omitted and therefore this case consists only in the coupling of the sea ice module to the ocean model. Note that the area covered by the ice shelves can eventually be occupied by sea ice in this simulation.

The model solutions have been saved daily and a model climatology (a mean year of 365 days) was constructed averaging the last 9 yr of simulations for all the experiments. These are compared in the next section.

## 3 Results

A rigorous model validation is limited by the scarcity of observations in this specific region of the global ocean. The lack of historical observations has slowed progress in understanding the Southern Ocean and its connections to the rest of the Earth system. The Southern Ocean, particularly under the ice shelves, is a typical example of where the spatiotemporal sampling is still poor despite all the recent efforts from the scientific community. The present analysis has the purpose of identifying the relative importance of

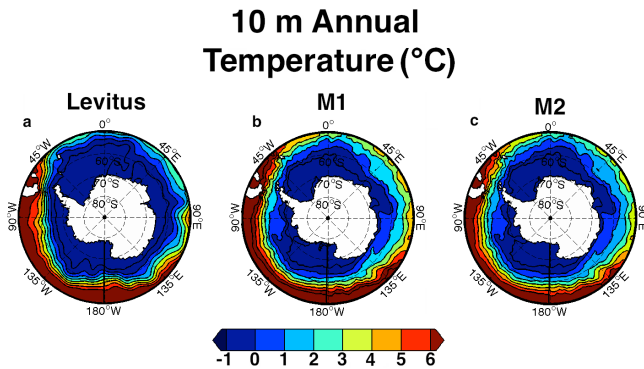


**Fig. 3.** Near surface (10 m) annual mean temperature fields in centigrade for (a) Levitus climatology, (b) M1, and (c) M2 simulations.

the cryosphere's components and their interactions with the Weddell Sea in the Southern Ocean. Therefore our analysis is focused on comparing the different experimental results rather than a robust validation against observations. Nonetheless, global databases such as Levitus World Ocean Data 1998 climatology, Simple Ocean Data Assimilation (SODA) and sea ice concentration derived from satellite data were used to perform a qualitative comparison with the model results. It should be noted that the Levitus dataset has a summer bias because it is the time of the year when most ships make measurements in the Southern Ocean.

### 3.1 Annual mean temperature and salinity

The annual mean fields of temperature and salinity were calculated for the four model climatologies. In order to be compared, the horizontal fields were linearly interpolated to standard  $z$  levels considering the bathymetry, the ice shelf thickness and the mean sea surface height. Figure 3 shows the annual mean temperature at 10 m for the Levitus 1998 climatology (Fig. 3a), experiments M1 (Fig. 3b) and M2 (Fig. 3c). The 10 m Levitus annual temperature, representative of upper levels, shows a clear latitudinal gradient along the model domain. In particular, higher gradients are observed towards the west of the Antarctic Peninsula (from 135° E to 45° W, clockwise) where temperature differences higher than 7 °C from 83° S to 50° S can be found. These features are well represented in every experiment, suggesting that the model adequately resolves the surface fluxes. No large qualitative differences between M1 and M2 experiments can be reported regarding temperature at the upper levels along the whole model domain.

The annual mean salinities at 10 m for Levitus 1998 climatology and the model results are shown in Fig. 4. The near surface salinity according to Levitus (Fig. 4a) presents the highest values in the Weddell Sea where the sea ice formation is a crucial process, and at low latitudes in the Pacific Ocean. This pattern is reproduced by the model in the M1 and M2 experiments (Fig. 4b, c).

### 10 m Annual Salinity

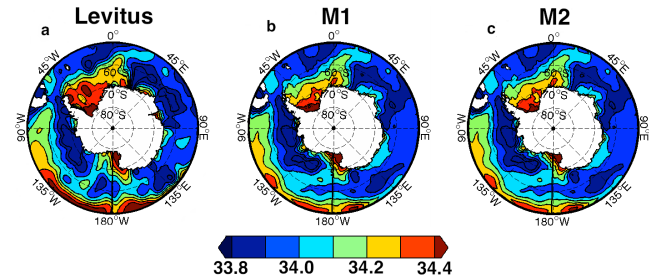


**Fig. 4.** Near surface (10 m) annual mean salinity for (a) Levitus climatology, (b) M1, and (c) M2.

To evaluate the local differences in temperature and salinity produced by the inclusion of the ice shelf, vertical sections were compared. Figure 5 shows the vertical sections of annual temperature (Fig. 5b) and salinity (Fig. 5c) along 40° W through the Filchner–Ronne Ice Shelf (Fig. 5a) for the Levitus and model climatologies. It can be seen that the model qualitatively reproduces the vertical Levitus thermohaline structure in experiments M1 and M2. In these cases, the ocean surface is covered by ice, accounting for the minimum values of temperature and salinity in the upper levels. Both variables increase their values with depth. Whereas modeled salinity compares well with Levitus, the model tends to underestimate temperature in lower levels.

To better compare the model experiments, Fig. 6 shows the vertical sections of annual temperature (Fig. 6b) and salinity (Fig. 6c) under the Ronne Ice Shelf in the Weddell Sea (57° W; Fig. 6a). It should be noted that ice shelves are not part of the Levitus climatology, therefore it cannot be compared to the model results. In M1 the ice thickness is prescribed and a layer of thickness 150–300 m is present under the ice shelf. It can be seen in Fig. 6 that the modeled temperature and salinity in M1 and M2 experiments are very similar in the northernmost part of the section but they are very different under the ice shelf, showing a reasonable configuration consistent with lower temperatures and higher salinities associated with ice-melt and brine rejection in experiment M1. The temperature values for M1 and M2 experiments range between  $-2.0$  and  $-1.75$  °C and salinities between 34.6 and 34.8 south of 76° S.

### 3.2 Annual mean circulation in the Weddell Sea

The Weddell Sea is characterized by a climatological low atmospheric pressure center that dominates the basin-scale ocean circulation. The Weddell Gyre extends from the Antarctic Peninsula to 30° E covering both Weddell and Enderby basins (Orsi et al., 1993). To the north it is bounded by the Antarctic Circumpolar Current and to the south by the continental shelf slope in the southern Weddell Sea. Since

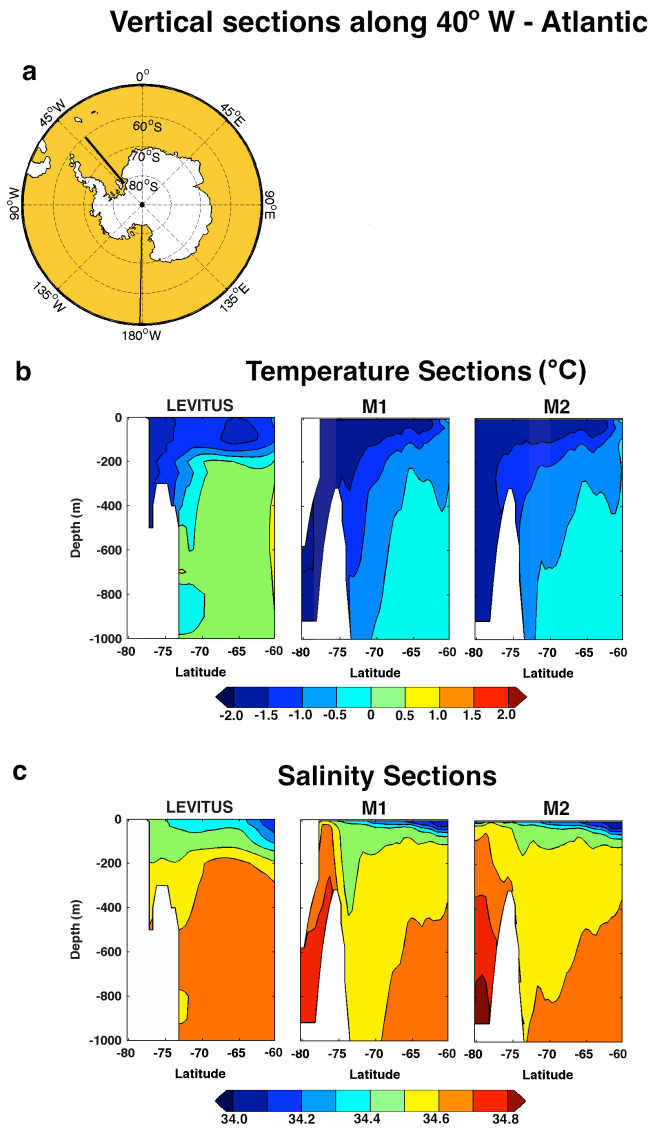


**Fig. 5.** Vertical sections along the Flichner–Ronne Ice Shelf at 40° W (a) of annual mean temperature (b) and salinity (c) for Levitus and model climatologies.

the vertical density gradients in the Weddell Sea are relatively small, sea surface height (SSH) can be used to describe depth integrated flow. Figure 7 shows, for the Weddell Sea, the annual mean SSH in meters together with the simulated barotropic currents modeled for the two experiments. Negative SSH values can be seen for both experiments. The minimum values for M1 and M2 are centered in the Weddell Sea, which shows that the Weddell Gyre is qualitatively well represented.

Transport of volume or mass can be established using the meridional overturning stream function. It is commonly used to sum up various features of the large-scale circulation, particularly the effects of the thermohaline forcing. The

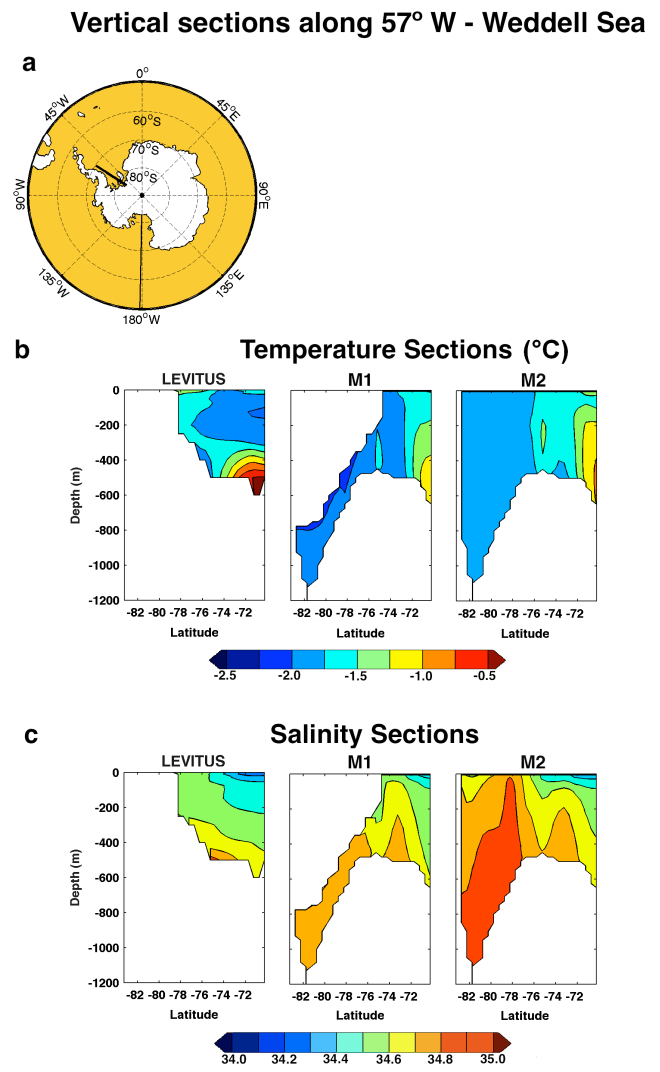


**Fig. 6.** Vertical sections along the Ronne Ice Shelf at 57° W (a) of the annual mean temperature (b) and salinity (c) for Levitus and model climatologies.

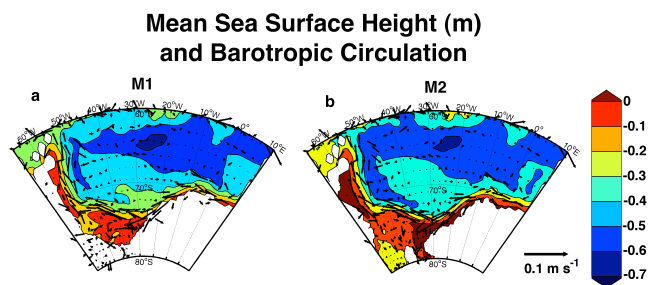


**Fig. 7.** Annual mean sea surface height in meters and barotropic circulation in the Weddell Sea for M1 (a) and M2 (b) experiments.

## Meridional Overturning Streamfunction ( $S_v$ ) in the Weddell Sea

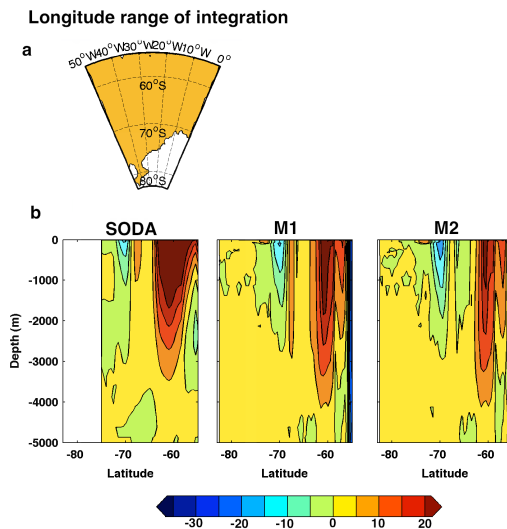


**Fig. 8.** Weddell Sea (a) annual mean meridional overturning circulation in Sverdrups for SODA, M1 and M2 simulation results.

meridional overturning streamfunction was computed for the Weddell Sea as follows:

$$\psi_{(x,y)} = - \int_{50^{\circ}W}^{0^{\circ}} \int_{H(x,y)}^z v dx dz, \quad (1)$$

where  $v$  is the meridional velocity, the vertical limits extend from the ocean bottom  $H$  to a depth  $z$ , and the zonal integral extends from  $50^{\circ}W$  to the Greenwich meridian. This computation was repeated for the four experiments and for the annual mean data obtained from the Simple Ocean Data Assimilation (SODA) dataset. SODA consists of an ocean reanalysis that provides an estimate of the evolving physical state of the ocean (Carton and Giese, 2008). The dataset obtained from SODA reanalysis represents a considerable improvement when compared to the existing hydrographic observations or even available numerical simulations in the analysis and diagnostic of ocean processes, in particular those related to water mass changes and variability. All available data from hydrographic stations, expandable bathythermographs (XBTs), altimetry and floats are assimilated into the model. Freshwater fluxes are determined from precipitation data of the Global Precipitation Climatology Project (available since 1979) and evaporation is calculated from bulk formulae. The surface heat flux is also calculated using bulk formulae.

The results are plotted in Fig. 8 as a function of latitude and depth. Results from experiments M1 and M2 compare reasonably well to SODA, Simulation of the Deacon cell, reaching values in excess of 20 Sv north of  $65^{\circ}S$  in response to the westerlies at  $60^{\circ}S$ , is well represented in M1 and

M2. In addition, both experiments are able to reproduce a coastal cell of approximately 10 Sv very close to Antarctica. The difference between the two experiments is very subtle where the strength of the circulation south of approximately  $65^{\circ}S$  is greater for M2 while north of it the circulation is stronger for M1, with its maximum extending below 2000 m. The presence of the ice shelf thermodynamics in experiment M1, changes the nature of the water mass interactions contributing to the displacement of the overturning circulation relative to M2.

### 3.3 Water masses identification in the Weddell Sea

Water masses act as important reservoirs of heat and salt acquiring their signatures from atmospheric processes near their formation zones and, consequently, they are excellent indicators of climatic change (Tomczak, 1999). Potential temperature–salinity diagrams were constructed to identify, for each model experiment, the Weddell Sea water masses. Figure 9 shows the diagrams derived from the annual mean temperature and salinity along  $40^{\circ}W$  of Levitus climatology and the two experiments. The boxes inside the  $T$ – $S$  diagram in Fig. 9a indicate the thermohaline limits for the typical water masses reported in the Weddell Sea. The Warm Deep Water (WDW), with  $0 < \theta < 1^{\circ}C$  and  $34.6 < S < 34.75$ , is a relatively warm and salty water found in the intermediate layers of the Weddell Sea (Carmack and Foster, 1975). The WDW can suffer mixing processes with the Antarctic Surface Water (AASW), the Winter Water (WW) and the Shelf Water (SW), producing the Modified Warm Deep Water (MWDW). This water mass, with temperature range between  $-1.7$  and  $-0.7^{\circ}C$  and salinity range between 34.4 and 34.6, has an important role in the AABW formation (Carmack and Foster, 1975). Below the WDW, the Weddell Sea presents two varieties of AABW: the Weddell Sea Deep Water (WSDW) with  $-0.7 < \theta < 0^{\circ}C$  and  $34.4 < S < 34.6$ , and the Weddell Sea Bottom Water (WSBW) with  $\theta < -0.7^{\circ}C$  and  $34.62 < S < 34.68$  (Carmack and Foster, 1975). Finally, the Ice Shelf Water (ISW;  $\theta < -1.9^{\circ}C$ ;  $34.20 < S < 34.70$ ; Kerr et al., 2012) is formed in the south of the Weddell Sea from the interactions of High Salinity Shelf Water (HSSW) and possibly Low Salinity Shelf Water (LSSW) with the ice shelf (Kerr et al., 2012).

Some of the features from the Levitus  $T$ – $S$  diagram are well reproduced by the M1 and M2 experiments. For instance, whereas the WDW is not captured by the model, the MWDW is present. Besides, the WSDW can be identified in both M1 and M2 experiments (Fig. 9b, c). The ISW is only present in the M1 experiment with a slight overestimation of salinity (of approximately 0.06), indicating the importance of the full representation of the ice shelves to reproduce this water mass.

### TS Diagrams along 40° W - Atlantic

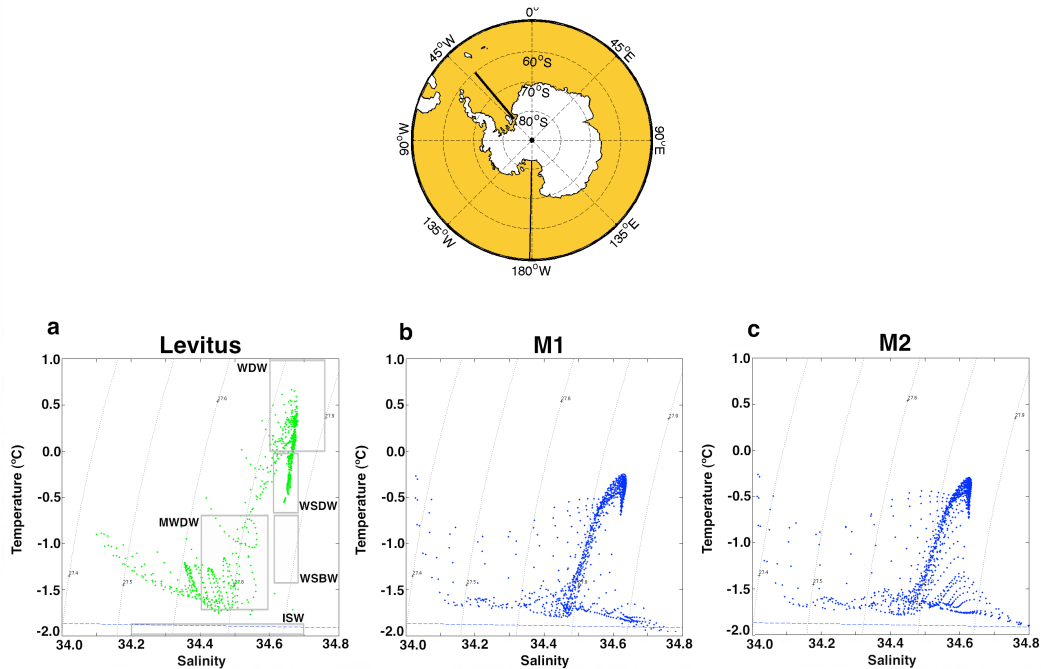


**Fig. 9.** *T–S* diagrams for the Weddell Sea along 40° W for the annual mean values of Levitus (a), M1 (b) and M2 (c) simulation results. The boxes inside the upper left panel indicate the thermohaline limits for the typical water masses reported in the Weddell Sea.

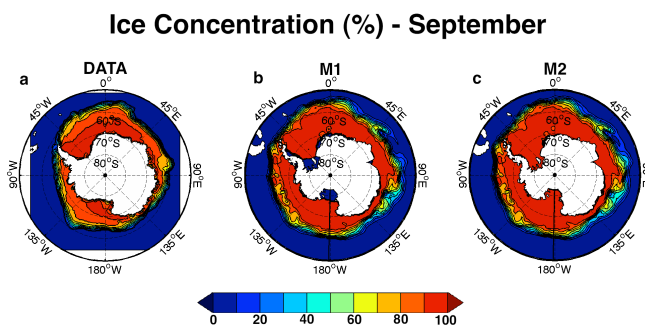


**Fig. 10.** Sea ice concentration in percentages for September (month of maximum sea ice coverage observed in the Southern Hemisphere) obtained from the (a) Nimbus-7 SMMR and DMSP SSM/I passive microwave data, (b) M1, and (c) M2 experiments.

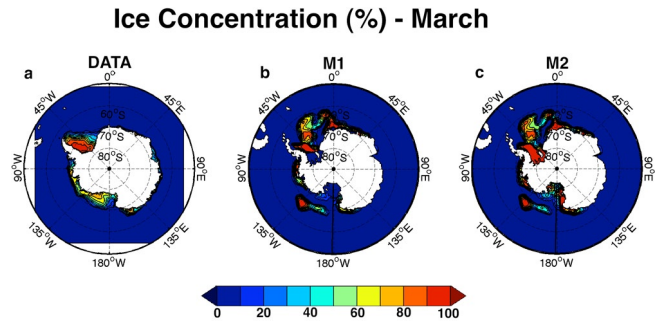


**Fig. 11.** Sea ice concentration in percentages for March (month of minimum sea ice coverage observed in the Southern Hemisphere) obtained from the (a) Nimbus-7 SMMR and DMSP SSM/I passive microwave data, (b) M1, and (c) M2 experiments.

#### 3.4 Seasonal sea ice cover

Sea ice concentration (area of sea ice per grid cell area) reflects the effects of dynamics and thermodynamic processes originating in the atmosphere–ocean–sea ice system. Thus, this variable is a good diagnostic of the model’s ability to reproduce near surface processes in high latitudes. Model results regarding the sea ice concentration are compared to satellite climatology from the Nimbus-7 SMMR and DMSP

SSM/I passive microwave data (Cavalieri et al., 1996, updated 2008) over the period 1979–2007. Figures 10 and 11 map the sea ice concentration (in percentage) for September (month of maximum sea ice coverage in the Southern Hemisphere) and March (month of minimum sea ice coverage), respectively, derived by the satellite data and the numerical experiments.

For the Southern Hemisphere’s wintertime (Fig. 10) all experiments show results that are in agreement with the

observations, which indicates a good parameterization of the surface fluxes. In particular, the horizontal pattern with a minimum latitudinal sea ice extension in the western Pacific, at approximately 135° E, and a maximum in the Weddell Sea are adequately represented by the model in all the simulations. Nevertheless, the model seems to overestimate the sea ice coverage in September. Model results for sea ice concentration differ very little between the experiments, which is an indication of how closely linked sea ice formation is to the surface atmospheric forcing. It is worthwhile to note that the area covered by the ice shelves is completely occupied by sea ice when they are turned off (M2 model experiment).

The observed sea ice concentration in March (Fig. 11a) shows an ocean free of sea ice in the eastern Atlantic, Indian and western Pacific oceans (approximately from the Greenwich Meridian to 160° E, clockwise), whereas the Weddell Sea, the eastern Pacific and the Ross Sea present covered areas. In particular the maximum ice concentration in summertime occurs to the east of the Antarctic Peninsula, where values of 100 % concentration are found. This last feature is captured by the model in the M1 and M2 experiments (Fig. 11b, c). Nevertheless the model overestimates the summer sea ice cover in the Weddell Sea and in general performs a poor representation around Antarctica.

#### 4 Conclusions

In this paper a thermodynamic active sea ice and ice shelf parameterization is used in a regional numerical model of the Southern Ocean. For the first time, ROMS was applied in a circumpolar domain with sea ice and ice shelf for climate-scale integrations. The relative importance of the different model components to obtain an adequate representation of the observed hydrography and circulation focusing on the Weddell Sea is evaluated. In particular, the effects of coupling an ice shelf parameterization with active thermodynamics is studied.

The ice shelves surrounding Antarctica play an important role in the formation of the Antarctic Bottom Water, and consequently they have to be represented in a realistic way to improve the understanding of the role of the Southern Ocean in global circulation and climate. Circulation beneath the ice shelves and the associated meltwater input have a profound impact on shelf water properties (Nicholls et al., 2009). In fact, poleward of the shelf break, 40 % of the sea surface is covered by floating ice shelves, which range in thickness from 100 to 2000 m, and can isolate the ocean from the atmosphere. Because of this, the interaction between the ice shelves and the ocean is a fundamental element of the climate system. We introduced them initially as a bathymetric surface alone and in a subsequent step the thermodynamic fluxes between the bottom of the ice and the ocean were considered.

Although model solutions underneath the ice shelves are difficult to validate due to the scarcity of observations, our results suggest that the thermodynamic fluxes between the ice shelf and the ocean must be considered in order to obtain representative hydrographic values under the ice shelves. The representation of the cryosphere–ocean processes, and hence dense water formation, is much more complex than having sea ice alone.

The results presented in this paper constitute a contribution to the development of a powerful tool in order to study the atmosphere–ocean–ice coupled system in the Southern Ocean. In particular, our interest is focused on the prediction of the system response to climate change scenarios and its implication on global climate. Ergo, our next step will be to study the interannual variability of the last 60 yr and the role of the tidal forcing in the ocean circulation and mixing. However, to provide a more comprehensive picture of these processes, a higher horizontal resolution model is needed, not only for the Weddell Sea but all around the circumpolar domain. As the processes in the Weddell Sea significantly influence the hydrography of the South Atlantic, the characteristics of the Ross Sea should be adequately considered since they would influence the hydrography in the South Pacific. Processes that occur in the open ocean also have to be considered. Consequently a combination of physical processes and refined model resolution may be needed to better understand the important interactions that take place within the continental shelf. Efforts are currently being devoted to implement an extended and higher resolution model domain.

*Acknowledgements.* This paper is a contribution to the Project INCT da Criosfera. Computational resources were provided by the NCAR, which is supported by the National Science Foundation. Meccia was supported by a postdoctoral fellowship awarded by the FAPESP. We also would like to thank Mike Dinniman for his help in implementing the thermodynamic component of the ice shelf in ROMS To CNPq and CAPES.

Edited by: R. Marsh

#### References

- Beckmann, A. and Goosse, H.: A parameterization of ice shelf–ocean interaction for climate models, *Ocean Model.*, 5, 157–170, 2003.
- Beckmann, A., Hellmer, H., and Timmermann, R.: A numerical model of the Weddell Sea: Large scale circulation and water mass distribution, *J. Geophys. Res.*, 104, 23374–23391, 1999.
- Budgell, W.: Numerical simulation of ice-ocean variability in the Barents Sea region, *Ocean Dynam.*, 55, 370–387, 2005.
- Carmack, E. and Foster, T.: On the flow of water out of the Weddell Sea, *Deep Sea Res. Ocean. Abstr.*, 22, 711–724, doi:10.1016/0011-7471(75)90077-7, 1975.
- Carton, J. and Giese, B.: A reanalysis of ocean climate using Simple Ocean Data Assimilation (SODA), *Mon. Weather Rev.*, 136, 2999–3017, 2008.

- Cavaliere, D., Parkinson, C., Gloersen, P., and Zwally, H.: Sea Ice Concentrations from Nimbus-7 SMMR and DMSP SSM/I-SSMIS Passive Microwave Data, [1979–2007], Boulder, Colorado USA: National Snow and Ice Data Center, Digital media, 1996, updated 2008.
- Deacon, G.: The hydrology of the Southern Ocean, vol. 15, Cambridge University Press, 1937.
- Dinniman, M., Klinck, J., and Smith Jr., W.: Influence of sea ice cover and icebergs on circulation and water mass formation in a numerical circulation model of the Ross Sea, Antarctica, *J. Geophys. Res.*, 112, C11013, doi:10.1029/2006JC004036, 2007.
- Fahrbach, E., Rohardt, G., Scheele, N., Schroder, M., Strass, V., and Wisotzki, A.: Formation and discharge of deep and bottom water in the northwestern Weddell Sea, *J. Marine Res.*, 53, 515–538, 1995.
- Fairall, C., Bradley, E., Hare, J., Grachev, A., and Edson, J.: Bulk parameterization of air-sea fluxes: Updates and verification for the COARE algorithm, *J. Climate*, 16, 571–591, 2003.
- Gill, A.: Circulation and bottom water production in the Weddell Sea, *Deep Sea Res. Ocean. Abstr.*, 20, 111–140, doi:10.1016/0011-7471(73)90048-X, 1973.
- Goosse, H. and Fichefet, T.: Importance of ice-ocean interactions for the global ocean circulation: A model study, *J. Geophys. Res.*, 104, 23337–23355, 1999.
- Griffies, S. M., Biastoch, A., Böning, C., Bryan, F., Danabasoglu, G., Chassignet, E. P., England, M. H., Gerdes, R., Haak, H., Hallberg, R. W., et al.: Coordinated ocean-ice reference experiments (COREs), *Ocean Model.*, 26, 1–46, 2009.
- Haidvogel, D., Wilkin, J., and Young, R.: A semi-spectral primitive equation ocean circulation model using vertical sigma and orthogonal curvilinear horizontal coordinates, *J. Comput. Phys.*, 94, 151–185, 1991.
- Haidvogel, D., Arango, H., Budgell, W., Cornuelle, B., Curchitser, E., Di Lorenzo, E., Fennel, K., Geyer, W., Hermann, A., Lanerolle, L., et al.: Ocean forecasting in terrain-following coordinates: Formulation and skill assessment of the Regional Ocean Modeling System, *J. Comput. Phys.*, 227, 3595–3624, 2008.
- Hellmer, H.: Impact of Antarctic ice shelf basal melting on sea ice and deep ocean properties, *Geophys. Res. Lett.*, 31, L10307, doi:10.1029/2004GL019506, 2004.
- Hellmer, H., Kauker, F., and Timmermann, R.: Weddell Sea anomalies: Excitation, propagation, and possible consequences, *Geophys. Res. Lett.*, 36, L12605, doi:10.1029/2009GL038407, 2009.
- Hellmer, H. H., Kauker, F., Timmermann, R., Determann, J., and Rae, J.: Twenty-first-century warming of a large Antarctic ice-shelf cavity by a redirected coastal current, *Nature*, 485, 225–228, 2012.
- Holland, D. and Jenkins, A.: Modeling thermodynamic ice-ocean interactions at the base of an ice shelf, *J. Phys. Oceanogr.*, 29, 1787–1800, 1999.
- Holland, P., Jenkins, A., and Holland, D.: The response of ice shelf basal melting to variations in ocean temperature, *J. Climate*, 21, 2558–2572, doi:10.1175/2007JCLI1909.1, 2008.
- Hunke, E.: Viscous-plastic sea ice dynamics with the EVP model: Linearization issues, *J. Comput. Phys.*, 170, 18–38, doi:10.1006/jcph.2001.6710, 2001.
- Jenkins, A.: A one-dimensional model of ice shelf-ocean interaction, *J. Geophys. Res.*, 96, 20671–20677, doi:10.1029/91JC01842, 1991.
- Jenkins, A. and Holland, D.: A model study of ocean circulation beneath Filchner-Ronne Ice Shelf, Antarctica: Implications for bottom water formation, *Geophys. Res. Lett.*, 29, 1193, doi:10.1029/2001GL014589, 2002.
- Kerr, R., Wainer, I., and Mata, M.: Representation of the Weddell Sea deep water masses in the ocean component of the NCAR-CCSM model, *Antarctic Science*, 21, 301–312, doi:10.1017/S0954102009001825, 2009.
- Kerr, R., Heywood, K. J., Mata, M. M., and Garcia, C. A. E.: On the outflow of dense water from the Weddell and Ross Seas in OCCAM model, *Ocean Sci.*, 8, 369–388, doi:10.5194/os-8-369-2012, 2012.
- Large, W. and Yeager, S.: The global climatology of an interannually varying air-sea flux data set, *Clim. Dynam.*, 33, 341–364, 2009.
- Losch, M.: Modeling ice shelf cavities in az coordinate ocean general circulation model, *J. Geophys. Res.*, 113, C08043, doi:10.1029/2007JC004368, 2008.
- Lythe, M., Vaughan, D., and the BEDMAP Consortium: BEDMAP: A new ice thickness and subglacial topographic model of Antarctica, *J. Geophys. Res.*, 106, 11335–11351, 2001.
- Matano, R., Gordon, A., Muench, R., and Palma, E.: A numerical study of the circulation in the northwestern Weddell Sea, *Deep Sea Res. Part II*, 49, 4827–4841, doi:10.1016/S0967-0645(02)00161-3, 2002.
- Mellor, G. and Kantha, L.: An ice-ocean coupled model, *J. Geophys. Res.*, 94, 10937–10954, 1989.
- NGDC: Data Announcement 88-MGG-02, Digital relief of the Surface of the Earth, NOAA, National Geophysical Data Center – NGDC, Boulder, Colorado, 1988.
- Nicholls, K., Østerhus, S., Makinson, K., Gammelsrød, T., and Fahrbach, E.: Ice-ocean processes over the continental shelf of the southern Weddell Sea, Antarctica: A review, *Rev. Geophys.*, 47, RG3003, doi:10.1029/2007RG000250, 2009.
- Orsi, A., Nowlin, W., and Whitworth, T.: On the circulation and stratification of the Weddell Gyre, *Deep-Sea Res. Part A*, 40, 169–203, 1993.
- Renner, A., Heywood, K., and Thorpe, S.: Validation of three global ocean models in the Weddell Sea, *Ocean Model.*, 30, 1–15, doi:10.1016/j.ocemod.2009.05.007, 2009.
- Rintoul, S., Sparrow, M., Meredith, M., Wadley, V., Speer, K., Hofmann, E., Summerhayes, C., Urban, E., and Bellerby, R.: The Southern Ocean Observing System, *Oceanography*, 25, 68–69, doi:10.5670/oceanog.2012.76, 2012.
- Shchepetkin, A. F. and McWilliams, J. C.: The regional oceanic modeling system (ROMS): a split-explicit, free-surface, topography-following-coordinate oceanic model, *Ocean Model.*, 9, 347–404, 2005.
- Smith, W. and Sandwell, D.: Global sea floor topography from satellite altimetry and ship depth soundings, *Science*, 277, 1956–1962, 1997.
- Song, Y. and Haidvogel, D.: A semi-implicit ocean circulation model using a generalized topography-following coordinate system, *J. Comput. Phys.*, 115, 228–244, 1994.
- Timmerman, R., Wang, Q., and Hellmer, H.: Ice shelf basal melting in a global finite-element sea ice-ice shelf-ocean model, *Ann. Glaciol.*, 53, 303–314, 2012.
- Timmermann, R., Beckmann, A., and Hellmer, H.: Simulation of ice-ocean dynamics in the Weddell Sea, Part I: Model

- configuration and validation, *J. Geophys. Res.*, 10, 3024, doi:10.1029/2000JC000741, 2002a.
- Timmermann, R., Hellmer, H., and Beckmann, A.: Simulations of ice-ocean dynamics in the Weddell Sea 2, Interannual variability 1985–1993, *J. Geophys. Res.*, 107, 3025, doi:10.1029/2000JC000742, 2002b.
- Tomczak, M.: Some historical, theoretical and applied aspects of quantitative water mass analysis, *J. Marine Res.*, 57, 275–303, 1999.
- Wilkin, J. and Hedstrom, K.: Users manual for an orthogonal curvilinear grid-generation package, Technical Report: Institute of Marine and Coastal Sciences, Rutgers University, New Brunswick, NJ, available at: [http://www.marine.rutgers.edu/po/tools/gridpak/grid\\_manual.ps.gz](http://www.marine.rutgers.edu/po/tools/gridpak/grid_manual.ps.gz) (last access: 10 November 2011), 1998.